A Comparative Analytical Study of Low-Level Motion Estimators in Space-Time Images

doi: 10.5281/zenodo.14887

Bernd Jähne[1,2]

[1] Interdisziplinäres Zentrum für Wissenschaftliches Rechnen (IWR)
Universität Heidelberg, Im Neuenheimer Feld 368, D-69120 Heidelberg
[2] Scripps Institution of Oceanography, University of California, San Diego
La Jolla, CA 92093-0230, USA, E-mail: bjaehne@ucsd.edu

Abstract. Various concepts for low-level motion estimation based on differential, tensor, and phase methods are revisited. They are reformulated in a unified way as filter methods in the continuous space-time domain. This approach allows inherent conceptual deficits to be distinguished from those related to the implementation in discrete space. A detailed analytical error analysis is performed. All techniques yield unbiased motion estimates for areas of constant velocity with *any* type of gray value structure in continuous space. Errors are only introduced by an inadequate discrete implementation. Further investigated are the influence of zero-mean normal distributed noise, spatially and temporally (accelerated) varying motion, motion discontinuities, and illumination changes.

1 Introduction

Recently, *Barron et al.* [4] pointed out the lack of quantitative evaluation for motion determination. In their paper they perform direct experimental comparisons of different techniques with the same set of scenes. Here a general *analytical* analysis of the different primitive motion estimators which does not depend on specific assumptions about the spatial gray value structures is performed. The common approach so far was to expand spatial gray value structures in a Taylor series to the first or second order.

The paper consists of three major parts. An introduction into image sequence processing in the continuous space-time domain is given in section 2. In section 3, differential, tensor-based, and phase-based techniques are reformulated and extended into a unified filter concept, while a detailed analytical study of these techniques is the topic of section 4.

2 Motion in Space-Time Images

Motion appears as orientation in space-time images [1, 2, 3]. The relation between orientation and the velocity is given by

$$\boldsymbol{u} = -\begin{bmatrix} \tan\varphi_1 \\ \tan\varphi_2 \end{bmatrix}. \tag{1}$$

The angles φ_1 and φ_2 are defined as the angle between the plane normal to the lines of constant gray values and the x_1 and x_2 axes.

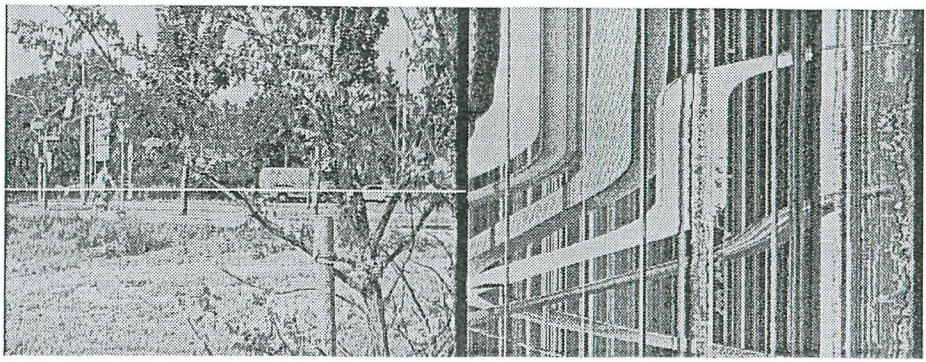

Fig. 1. *Complex traffic image sequence (taken at the city limits of Hanau, Germany) with multiple occlusions to illustrate how motion shows up in space time images: a) last image of the sequence; b) xt cross section at the marked line in a); the time axis spans 20.5 s, running downwards.*

The space-time slices of the traffic scene shown in figure 1 illustrate spatio-temporal gray value structures. All orientation changes due to not constant motion which can be seen in this sequence, take place only gradually because of the inertia of the objects. In contrast, occlusions are directly associated with sharp discontinuities of local orientation in the xt space.

The basic conceptional difference to approaches using two consecutive images is that the velocity is estimated *directly as orientation* in continuous space-time images and not as a discrete *displacement* between two images. These two concepts differ more than it appears at first glance. Algorithms for motion estimation can now be formulated in *continuous* xt space. This opens the way for a comparative analytical study of the different motion estimators. The following three general classes of gray value structures are employed:

$$\begin{array}{ll} \text{constant 1-D motion} & g(x - ut) \\ \text{planar wave, moving "edge"} & g(k^T x - \omega t) \\ \text{constant 2-D motion, moving "corner"} & g(x - ut) \end{array} \tag{2}$$

These elementary classes will also be modified systematically to include not constant motion in time, inhomogeneous motion including first-order spatial derivatives of the motion field, motion discontinuity (neighboring regions with different but constant motion), illumination changes, and zero-mean, normal-distributed noise.

There are significant advantages of this approach. First, no specific assumptions are made about the *spatial* structure of the gray values, except that they fall in one of the classes discussed above. Therefore the results are generally valid

in contrast to those based on the common approach that use Taylor expansions of the spatial gray value structure. Second, the performance of the different algorithms is determined in a unified and systematic way. The results with different schemes can be compared directly. Third, the different techniques are evaluated analytically *before* they are implemented in the discrete space. In this way, the errors inherent to the method can be separated from errors introduced by the discretization.

3 Formulation as Filter Methods in Space-Time Images

In this section several major approaches for image sequence processing are reformulated under the unified concept of filter operations in space-time images that can be combined as a sequence of the simple linear convolution and nonlinear point operations. This approach has also the advantage that the interrelations between the different concepts become more transparent.

3.1 Differential Methods

The classical differential methods based on first-order derivatives try to solve the aperture problem expressed in the brightness continuity constraint equation (BCCE)

$$\frac{\partial g}{\partial t} + \boldsymbol{f}^T \nabla g = 0 \tag{3}$$

by assuming a constant velocity in a neighborhood and using a least squares approach for N points in this neighborhood results in the equation

$$\tilde{\boldsymbol{f}} = (\boldsymbol{G}^T\boldsymbol{G})^{-1}\boldsymbol{g}_t \quad \text{with} \quad \boldsymbol{G} = \begin{bmatrix} G_{xx} & G_{xy} \\ G_{xy} & G_{yy} \end{bmatrix} \quad \text{and} \quad G_{pq} = \sum_{k=1}^{N} g_p(k) g_q(k), \tag{4}$$

provided that the 2×2-matrix $\boldsymbol{G}^T\boldsymbol{G}$ is invertible. (The expression g_p denotes a partial derivative of g in the direction p.) The resulting optical flow is denoted by the vector $\boldsymbol{f} = (e, f)$ and strictly distinguished from the projected motion field $\boldsymbol{u} = (u, v)$, since both may be different.

The least squares approach for the differential method can easily be reformulated to incorporate a more general smoothing. We can rewrite (4) and obtain

$$G_{kl}(\boldsymbol{x}, t) = \int_{-\infty}^{\infty} \mathrm{d}^2x' \, \mathrm{d}t' \; h(\boldsymbol{x} - \boldsymbol{x}', t - t') g_k(\boldsymbol{x}', t') g_l(\boldsymbol{x}', t') = \langle g_k g_l \rangle \,. \tag{5}$$

The term G_{kl} at the point $\boldsymbol{x}$ is obtained by convolving the product of the two corresponding partial derivatives with the smoothing kernel h centered at $\boldsymbol{x}$. For convolutions as in (5), we will use in the following the abbreviation $\langle \ldots \rangle$, as shown in (5). It is also important to note that the smoothing is extended into the temporal domain.

In a similar way, the differential geometric methods using second-order derivatives [11] can be extended to a filter method in the xt space:

$$\begin{bmatrix} \langle g_{xx} \rangle & \langle g_{xy} \rangle \\ \langle g_{xy} \rangle & \langle g_{yy} \rangle \end{bmatrix} \begin{bmatrix} e \\ f \end{bmatrix} = - \begin{bmatrix} \langle g_{xt} \rangle \\ \langle g_{yt} \rangle \end{bmatrix}. \tag{6}$$

This equation exactly corresponds to the result obtained by *Girosi et al.* [9]. He has derived it by applying the continuity of the optical flow (3) to two feature images, namely the horizontal and vertical spatial derivative:

$$f^T \nabla g_x + \frac{\partial g_x}{\partial t} = 0 \quad \text{and} \quad f^T \nabla g_y + \frac{\partial g_y}{\partial t} = 0. \tag{7}$$

In this way we come to an important generalization of the differential method. We can apply any preprocessing of the images, or can extract arbitrary feature images. The original, horizontal and vertical derivative images may be just regarded as a special case how more features to determine optical flow can be obtained from one image.

3.2 Tensor Methods

Knutsson [19] showed that local structure in an n-dimensional space can be represented by a symmetric $n \times n$ tensor

$$\boldsymbol{J}'(\boldsymbol{x}) = \langle \nabla g \nabla^T g \rangle. \tag{8}$$

These equations give a tensor representation of the local structure centered at the point $\boldsymbol{x}$ in the image. The components of the tensor are the same as for the filter formulation of the differential method. Local orientation, and thus optical flow, is now, however, solved by an eigenvalue analysis of the tensor.

In 2-D space, the result of the eigenvalue analysis can readily be given [13]. The 1-D optical flow f and the coherency are given by

$$f = -\tan\left(\frac{1}{2}\arctan\frac{2\langle g_x g_t \rangle}{\langle g_x^2 \rangle - \langle g_t^2 \rangle}\right), \quad c^2 = \frac{\left(\langle g_x^2 \rangle - \langle g_t^2 \rangle\right)^2 + 4\langle g_x g_t \rangle^2}{\left(\langle g_x^2 \rangle + \langle g_t^2 \rangle\right)^2}. \tag{9}$$

The coherency c is one for ideal local orientation (constant motion) and zero for distributed orientation. An equivalent approach [5] uses the inertia tensor:

$$J_{pp}(\boldsymbol{x}) = \sum_{q \neq p} \langle g_q^2 \rangle \quad \text{and} \quad J_{pq}(\boldsymbol{x}) = -\langle g_p g_q \rangle \tag{10}$$

This tensor has the same eigenvectors as the structure tensor and thus the same solutions. There are techniques which start from completely different ideas but end up with the same results. *Kass and Witkin's* [15] approach of directional filtering, for example, is identical to the general inertia tensor method [13]. They used a DoG filter as a special type of derivative filters. Without being aware of either *Bigün and Grandlund's* [5] earlier and *Knutsson's* [19] simultaneous work, *Rao and Schunck* [22] and *Rao* [21] proposed a moment-based technique that is equivalent to the structure tensor method.

3.3 Phase Methods

Fleet [6] and *Fleet and Jepson* [8] proposed the use of the phase for the computation of optical flow. The phase method is not appropriate to handle two-dimensional shifts, it is essentially a 1-D concept which measures the motion of a linearly oriented structure, a planar wave, in the direction of the gray value gradients. From this fact, *Fleet and Jepson* [7] derived a new paradigm for motion analysis. The image is decomposed with directional filters and in each of the components *normal velocities* are determined. The 2-D motion field is then composed from these normal velocities.

Computing the temporal and spatial derivatives of the phase, i. e., the gradient in the xt space, yields both the wave number and the frequency of the moving periodic structure

$$\nabla_{xt}\phi = \begin{bmatrix} \frac{\partial\phi}{\partial x} \\ \frac{\partial\phi}{\partial t} \end{bmatrix} = \begin{bmatrix} k \\ -\omega \end{bmatrix} \tag{11}$$

and the velocity is given as the ratio of the frequency to the wave number

$$u = \frac{\omega}{k} = -\frac{\partial\phi}{\partial t} \Big/ \frac{\partial\phi}{\partial x} \,. \tag{12}$$

Fleet and Jepson [7] use a set of Gabor filters for the directional composition. Gabor filters are quadrature filters with a shifted Gaussian-shaped transfer function. Fleet and Jepson used six directional filters with an angle resolution of 30° and a bandwidth of 0.8 octaves.

The phase can directly be computed from quadrature filter pairs. If the result from the filtering with the quadrature filter pair is denoted by q_+ and q_-, the phase is given by

$$\phi(\boldsymbol{x}, t) = \arctan\frac{q_-(\boldsymbol{x}, t)}{q_+(\boldsymbol{x}, t)}. \tag{13}$$

Using (12), the optical flow is

$${}^{p}f = -\frac{q_+ \dfrac{\partial q_-}{\partial t} - q_- \dfrac{\partial q_+}{\partial t}}{q_+ \dfrac{\partial q_-}{\partial x} - q_- \dfrac{\partial q_+}{\partial x}}. \tag{14}$$

Jähne [13, 14] proposed an alternative approach using a *directio-pyramidal decomposition* [10, 11] and Hilbert filtering to generate a second signal with a phase shift of $\pi/2$. Using a Hilbert filter and applying additional spatio-temporal smoothing, we can rewrite (14) and obtain

$${}^{p}f = -\frac{\langle {}^{e}g\,{}^{o}g_t - {}^{o}g\,{}^{e}g_t \rangle}{\langle {}^{e}g\,{}^{o}g_x - {}^{o}g\,{}^{e}g_x \rangle}, \tag{15}$$

where the original and Hilbert filtered signal are denoted with ${}^{e}g(x,t)$ and ${}^{o}g(x,t)$.

4 Analytical Studies

Because of limited space, only the results and their interpretation can be presented. Most of the proofs are omitted. Also not every type of patterns is studied for every technique. The missing proofs and a more detailed study can be found in [13].

4.1 Constant Motion in Noise-Free Image Sequences

In order to study this condition, an *arbitrary* spatial gray value structure moving with a constant velocity, $g'(\boldsymbol{x}, t) = g(\boldsymbol{x} - \boldsymbol{u}t)$ is used. All techniques gave exact, unbiased results in this case, i. e., $\boldsymbol{f} == \boldsymbol{u}$. This result is significant since they do not depend at all on the *specific form* of the gray value structure. Further remarks illustrate some finer points of the different techniques.

Differential Method. A solution exists only if the inverse of $\langle \nabla g \nabla^T g \rangle$ exists. This is the well known aperture problem. The widespread misconception that the gradient or differential methods deliver no accurate results when the spatial gray value structure cannot adequately be approximated by a first-order Taylor series (see, e. g., *Kearney et al.* [17]) is clearly contradicted by the above result.

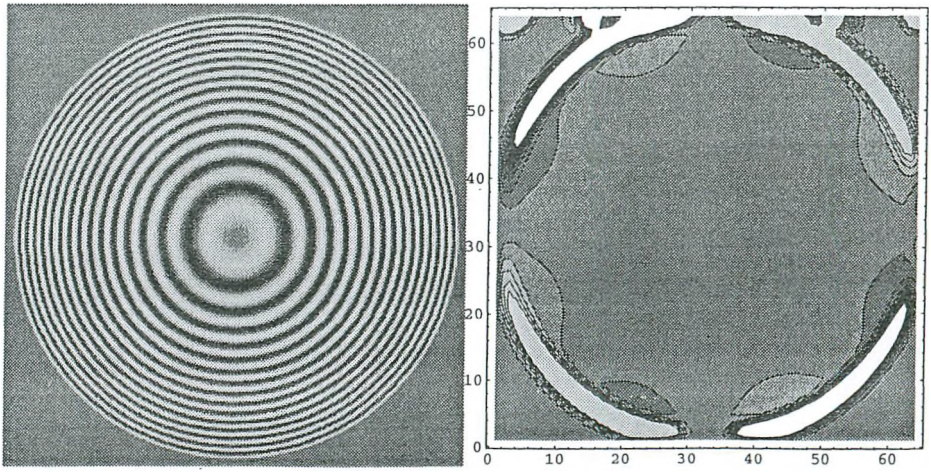

Fig. 2. *a) Synthetic image to test 1-D motion algorithms: concentric rings, the wave number is proportional to the distance from the center, minimal wavelength: 4 pixel at the outer edge. b) Test of the tensor algorithm using a B-spline-based derivative operator. Shown is a contour plot of the difference between the true and computed angle; the distance of the contour lines is 0.02, the range is -0.1 to 0.1.*

Errors are only introduced by the discrete implementation. Especially the choice of suitable spatial derivative operators is critical. This fact is illustrated by computing the orientation of a test image with concentric ring pattern as shown in figure 2a with the tensor-based method using a B-spline-based derivative filter.

The deviation of the computed from the true orientation is given in radian. This measure is also useful with respect to motion analysis since, for small values, it is equal to the tangent and thus directly expresses the velocity or velocity deviation of the displacement in pixels between two consecutive images. For all except the highest wave numbers at the very edge of the ring pattern, the deviation in orientation is less than 0.02 (1.2°). This constitutes a performance improvement of more than a factor of 10 over the symmetrical derivative operator ${}^{(1)}\mathcal{D}$ $(1/2\,(1\ 0\ -1))$, which shows deviations up to 0.3 (17°).

Phase Method. The puzzling fact for the phase method is that exact results do not depend on the fact that ${}^{o}g$ and ${}^{o}g$ are a Hilbert pair. It is sufficient that $e = \langle {}^{e}g\,{}^{o}g_x - {}^{o}g\,{}^{e}g_x \rangle \neq 0$. Consequently, the phase method gives accurate results with any pair of ${}^{e}g$ and ${}^{o}g$ provided that e is sufficiently large. A Hilbert pair, however, will still be optimal, since it maximizes e and minimizes the spatial variations in e. This result is also important considering the fact that it is difficult to design an effective wide-band Hilbert filter, since already a rough approximation will give good results.

4.2 Constant Motion in Noisy Image Sequences

Now zero-mean noise is added: $g'(x,t) = g(x-ut)+n(x,t)$ with $\langle n \rangle = 0, \langle n_t n_x \rangle = 0, \langle g_p n_q \rangle = 0$, i. e., and it is assumed that the partial derivatives of the noise function are not correlated with themselves or the partial derivatives of the image patterns.

Differential Method. In the 2-D case, we obtain

$$f = u(\langle \nabla g \nabla^T g \rangle + \langle \nabla n \nabla^T n \rangle)^{-1} \langle \nabla g \nabla^T g \rangle .$$

The matrix containing the mean squared gradients of the noise is a positive definite diagonal matrix. Thus the estimate of optical flow is biased by noise towards lower values both in the 1-D and 2-D case.

Tensor Method. The tensor method gives exact results even with noisy image sequences in the 1-D and 2-D case. In the 1-D case the coherency is

$$c^2 = \frac{\langle g_x^2 \rangle (1+u^2)}{\langle g_x^2 \rangle (1+u^2) + \langle n_x^2 \rangle + \langle n_t^2 \rangle}.$$

Thus the tensor method has two significant advantages over the differential method. First, the velocity estimate is not biased in noisy images provided that the noise is isotropic in the xt space, $\langle n_x^2 \rangle = \langle n_t^2 \rangle$. Second, the coherency is a direct measure for the signal to noise ratio in the image for constant motion.

4.3 Accelerated Motion

Again, we take a very general approach and introduce a first-order Taylor expansion of the motion field $g'(x,t) = g(x-(u+u_x x+u_t t)t)$. We further assume that $\langle t\rangle = \langle x\rangle = 0$ and introduce the abbreviation $\langle\cdot\rangle_g$ for an average weighted by the magnitude of the spatial gradient, $\langle\cdot g_x^2\rangle / \langle g_x^2\rangle$. Then $g'_x = g_x(1-u_x t)$, $g'_t = g_x(-u-u_x x-2u_t t)$.

Differential Method. The differential method gives the following result:

$$f = u + u_x \langle x\rangle_g + 2u_t \langle t\rangle_g - u_x^2 \langle xt\rangle_g + 2u_x u_t \langle t^2\rangle_g .$$

There are two types of bias terms. The first three terms are unequal to zero only when the square gradient is not evenly distributed in the neighborhood. Only the last term results in a bias even if the gradients are evenly distributed, but only if the velocity changes both in space and time. Thus it is a small second-order term.

Tensor Method. For the tensor method, only the coherency measure is analyzed for accelerated motion that is spatially homogeneous. The result is:

$$c \approx 1 - \frac{u_t^2 \langle t^2\rangle_g}{(1+u^2)^2}.$$

The coherency decrease is proportional to the acceleration squared (u_t^2) and only a small term. Thus the coherency is not sensitive to *gradual* changes in the velocity.

4.4 Motion Discontinuity

Next, we turn to the analysis of motion discontinuities. We take two subareas within the neighborhood with different velocities. Without loss of generality, we choose $g'(x,t) = g(x+ut)\Pi(-x)$ and $g''(x,t) = g(x-ut)\Pi(x)$, where $\Pi(x)$ is the step function (we can gain all other cases by rotation of the coordinate system). Then the estimate for the optical flow is

$$f \approx u \frac{\left\langle g'^2_x\right\rangle - \left\langle g''^2_x\right\rangle}{\left\langle g'^2_x\right\rangle + \left\langle g''^2_x\right\rangle}.$$

If the mean square gradient is equal in both regions, the estimated optical flow is zero as expected. The coherency is

$$c^2 = 1 - 2\gamma \sin^2 \alpha/2, \tag{16}$$

where α is the angle between the spatio-temporal orientation in the two regions (which is related by $\tan(\alpha/2) = u$ to the velocity in the two regions) and γ is a measure that compares the mean square gradient in the two regions

$$\gamma = 1 - \left(\frac{\left\langle g'^2_x \right\rangle - \left\langle g''^2_x \right\rangle}{\left\langle g'^2_x \right\rangle + \left\langle g''^2_x \right\rangle} \right).$$

It is one if both regions have the same mean square gradient and zero if the mean square gradient in one region is significantly larger than in the other. If the mean square gradients in both regions are equal, the expression for the coherency becomes even simpler: $c = \cos\alpha$. This tells us that the coherency is zero if the orientations in the two regions are orthogonal.

4.5 Illumination change

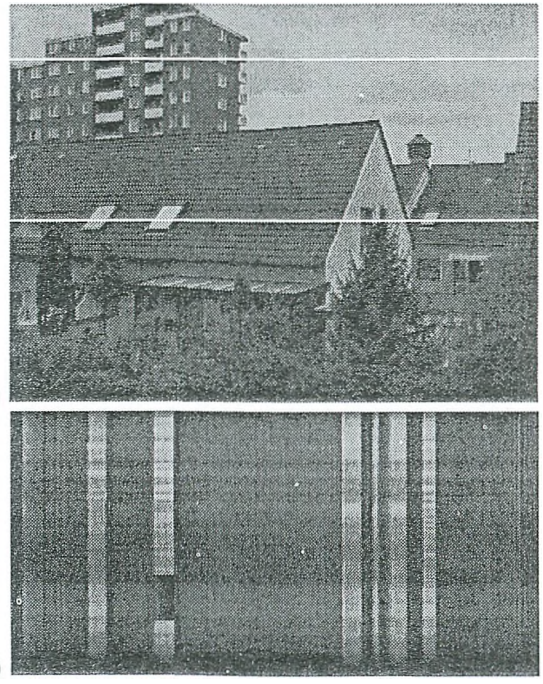

Fig. 3. *Static scene with illumination changes only: a) first image of the sequence; b) xt cross section at the lower white line in a); the time axis spans 3.4 h, running downwards.*

Finally, we discuss the influence of illumination changes using $g'(x,t) = g(x - ut, t)$. Then $g'_x = g_x$ and $g'_t = -ug_x + g_t$, where g_t means the explicit temporal

derivative. The estimate of the optical flow gives

$$f = \frac{u - \langle g_x g_t \rangle / \langle {g_x}^2 \rangle}{1 - u^2 + 2u \langle g_x g_t \rangle / \langle {g_x}^2 \rangle - \langle {g_t}^2 \rangle / \langle {g_x}^2 \rangle}.$$

Even if $\langle g_x g_t \rangle = 0$, the velocity estimate is biased towards higher velocities, as can be seen for small u:

$$f = \frac{u}{1 - \langle {g_t}^2 \rangle / \langle {g_x}^2 \rangle}.$$

This result is not surprising, since illumination changes occur as additional oriented patterns with an orientation corresponding to infinite velocity (figure 3). Since we know, however, that these patterns cannot be caused by motion, they can be removed by an appropriate directional filter.

5 Conclusions and Outlook

A unified concept for methods based on differential, tensor, and phase method that compute optical flow directly in space time images has been presented. All the estimators are composed of simple convolution kernels (binomial smoothing, first-order derivatives, and — only for the phase method — a Hilbert filter) and nonlinear point operators (pointwise image multiplication). All methods yield unbiased results in regions of constant motion. However, they differ in the response to less perfect regions. The differential method has the significant disadvantage that the motion estimation is biased by noise. An important piece of future work would be the comparison of the direct methods reported here with the quadrature filter set techniques established by Granlund's research group [18].

Acknowledgements

Financial support of this research by the Office of Naval Research (N00014-89-J-3222) is gratefully acknowledged. The major part of this research has been performed during guest professorships in the winter terms 1990/91 and 1991/92 at the Interdisciplinary Research Center for Scientific Computing (IWR) of Heidelberg University. I cordially thank Willi Jäger, director of the IWR, for his hospitality. The research reported here is part of my habilitation thesis in Applied Computer Science. I would like to thank Hans Burkhardt cordially for his interest in my research and the opportunity to submit my habilitation thesis to the Forschungsschwerpunkt "Informations- und Kommunikationstechnik" at the Technical University of Hamburg-Harburg in October 1991.

References

1. Adelson, E. H., and J. R. Bergen, Spatio-temporal energy models for the perception of motion, *J. Opt. Soc. Am.*, *73*, 1861, 1983.

2. Adelson, E. H., and J. R. Bergen, Spatiotemporal energy models for the perception of motion, *J. Opt. Soc. Am., A 2*, 284–299, 1985.
3. Adelson, E. H., and J. R. Bergen, The extraction of spatio-temporal energy in human and machine vision, In *Proc. on Motion: Representation and Analysis*, Charleston, 1986, pp. 151–155, IEEE Computer Society Press, Washington, 1986.
4. Barron, J. L., D. J. Fleet, S. S. Beauchemin, and T. A. Burkitt, Performance of optical Flow Techniques, *Proc. Conf. Computer Vision and Pattern Recognition 1992 (CVPR'92)*, pp. 236–242, IEEE Comp. Soc., Washington DC, 1992.
5. Bigün, J., and G. H. Granlund, Optimal orientation detection of linear symmetry, *Proc. 1st Int. Conf. Comp. Vis.*, London 1987, pp. 433–438, IEEE Computer Society Press, Washington, 1987.
6. Fleet, D. J., *Measurement of image velocity*, Ph. D. Diss., University of Toronto, 1990.
7. Fleet, D. J., and A. D. Jepson, Hierarchical construction of orientation and velocity selective filters, *IEEE Trans. PAMI*, *11*, 315–325, 1989.
8. Fleet, D. J., and A. D. Jepson, Computation of component image velocity from local phase information, *Int. J. Comp. Vision*, 5, 77–104, 1990.
9. Girosi, F., A. Verri, and V. Torre, Constraints for the computation of optical flow, *Proc. Workshop on Visual Motion*, Irvine, CA, March 20–22, 1989, IEEE Comp. Soc. Washington DC, pp. 116–124, 1989.
10. Jähne, B., Image sequence analysis of complex physical objects: nonlinear small scale water surface waves, *Proc. 1st Int. Conf. Computer Vision (ICCV'87)*, London, pp. 191–200, IEEE Computer Society Press, Washington, 1987.
11. Jähne, B., *Digitale Bildverarbeitung*, Springer, Berlin, 1989.
12. Jähne, B., *Digital Image Processing — Concepts, Algorithms, and Scientific Applications*, 2nd edition, Springer, Berlin, 1993a.
13. Jähne, B., *Spatio-Temporal Image Processing, Theory and Scientific Applications*, Lecture Notes in Computer Science, Vol. 751, Springer, Berlin, 1993b.
14. Jähne, B., Analytical studies of low-level motion estimators in space-time images using a unified filter concept, *Proc. Comp. Vision & Pattern Recogn. (CVPR'94)*, Seattle, , IEEE Computer Society Press, Washington, 1994, in press.
15. Kass, M., and A. Witkin, Analyzing oriented patterns, *9th Int. Joint Conf. on Artificial Intelligence*, pp. 18–23, Los Angeles, CA, 1985.
16. Kass, M., and A. Witkin, Analyzing oriented patterns, *Computer Vision, Graphics and Pattern Recognition*, *37*, 362–385, 1987.
17. Kearney, J. K., W. B. Thompson, and D. L. Boley, Optical flow estimation: an error analysis of gradient-based methods with local optimization, *IEEE Trans. PAMI*, *9*, 229–244, 1987.
18. Knutsson, H., *Filtering and reconstruction in image processing*, Diss., Linköping Univ., 1982.
19. Knutsson, H., Representing local structure using tensors, *6th Scandinavian Conf. Image Analysis*, Oulu, Finland, 244–251, 1989.
20. Lim, J. S., *Two-dimensional signal and image processing*, Prentice-Hall, Englewood Cliffs, NJ, 1990.
21. Rao, A. R., *A Taxonomy for Texture Description and Identification*, Springer, New York, 1990.
22. Rao, A. R., and B. G. Schunck, Computing oriented texture fields, *Proc. Conf. Computer Vision and Pattern Recognition 1989 (CVPR'89)*, pp. 61–68, IEEE Comp. Soc., Washington DC, 1989.